Semiautomated Identification of the Phase Diagram for Enantiotropic Crystallizations using ATR-FTIR Spectroscopy and Laser Backscattering

Nicholas C. S. Kee,[†,‡,§] Reginald B. H. Tan,[‡,§] and Richard D. Braatz*[,†,||]

University of Illinois at Urbana−Champaign, 600 South Mathews Avenue, Urbana, Illinois 61801, United States of America; Department of Chemical and Biomolecular Engineering, National University of Singapore, 4 Engineering Drive 4, Singapore 117576; Institute of Chemical and Engineering Sciences, 1 Pesek Road, Jurong Island, Singapore 627833; and Department of Chemical Engineering, Massachusetts Institute of Technology, 77 Massachusetts Avenue, Cambridge, Massachusetts 02139, United States of America

A semiautomated procedure for measuring the phase diagram for enantiotropes in a dimorphic system was developed using Attenuated Total Reflection-Fourier Transform Infrared (ATR-FTIR) spectroscopy and laser backscattering (Focused Beam Reflectance Measurement, FBRM) for in situ measurement of solute concentration and the particle counts, respectively. The approach is demonstrated using L-phenylalanine, an enantiotropic pseudodimorph. The procedure involves the determination of the anhydrate-form solubility from in situ infrared spectroscopy of an equilibrated slurry, followed by the dissolution of the anhydrate form by heating. The monohydrate form is then recrystallized, and its solubility determined from slow heating until complete dissolution is detected by FBRM. The cycle is repeated for higher temperatures after addition of anhydrate crystals to create a slurry. The solubility of the monohydrate form was determined differently from the anhydrate form due to the interference on the infrared measurements from small needle-like monohydrate crystals. This single-experiment approach is expected to be applicable to other enantiotropic dimorph systems for the measurement of the phase diagram in a more efficient manner.

Introduction

Establishing the phase diagram is important for selective crystallization of specific polymorphs or solvates (also called *pseudopolymorphs*). The solubility curves and/or metastable limit can be used to define suitable crystallization domains for the crystallization of the desired crystal form.[1−3] Due to its influence on bioavailability, the solubility is important in the development of drug compounds.[4,5] The relative solubility of the forms is indicative of their thermodynamic stability, with the more stable form having lower solubility. For dimorphic systems, the solubility curves are classified as monotropic or enantiotropic. In monotropic systems, one form is consistently more stable (its solubility is always lower) at any temperature, while for an enantiotropic system, the stability is dependent on the temperature relative to the point of intersection between the solubility curves (see Figure 1). The temperature at the intersection, called the transition temperature, is important for drug development[6] because the suitable form for development and subsequent production is usually decided based on thermodynamic stability. The transition temperature can be estimated by linear extrapolation of van't Hoff plots for each form to find the point of intersection,[7,8] or by using the heats of solution and solubility data.[9]

The solubility is commonly determined using gravimetric techniques; a known amount of solid is added to a specific amount of solvent and maintained at a fixed temperature with constant stirring for sufficient time to reach equilibrium. The solubility is then calculated by subtracting the weight of the remaining solid phase (isolated by filtration) from its initial mass[10] or from the filtered liquid samples by solvent evaporation and measuring the weight of the "dry residue" mass.[11,12] Alternatively, liquid samples from equilibrated slurries can be evaluated with high-performance liquid chromatography (HPLC) systems.[13,14] These methods have been applied in polymorphic/pseudopolymorphic systems such as L-phenylalanine,[10] L-glutamic acid,[11] p-aminobenzoic acid,[12] L-serine,[13] and taltirelline.[14]

There has been an increased interest in a more automated approach to reduce the time and labor involved in solubility measurements. Some studies[15,16] have used in situ laser backscattering (Focused Beam Reflectance Measurement, FBRM)[17] to determine the solubility, based on the number of crystals counted per second. By slowly increasing the temperature of a slurry of known solute concentration, the saturation temperature can be determined as the point where the crystal counts decrease to zero indicating complete dissolution.[15] In another work,[16] the temperature at zero counts/sec was plotted against different heating rates, and the saturation temperature was determined by extrapolation to an infinitely slow heating rate. Both of these studies presented an automated scheme of measuring the

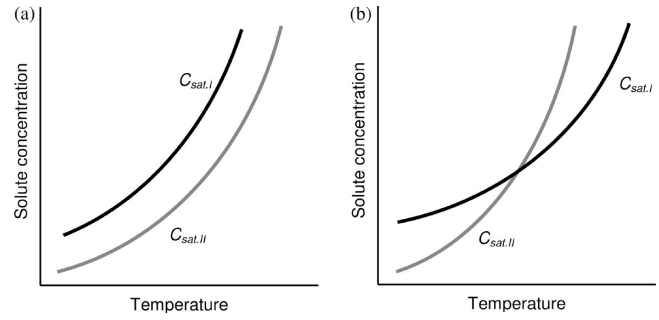

Figure 1. Solubility curves of dimorphs I and II ($C_{sat,I}$ and $C_{sat,II}$, respectively) in a (a) monotropic system and (b) enantiotropic system.

* To whom correspondence should be addressed. Phone: 617-253-3112. Fax: 617-258-0546. E-mail: braatz@mit.edu.
† University of Illinois at Urbana−Champaign.
‡ Department of Chemical and Biomolecular Engineering, National University of Singapore.
§ Institute of Chemical and Engineering Sciences.
|| Department of Chemical Engineering, Massachusetts Institute of Technology.

10.1021/ie100794h
Published on Web 11/24/2010

solubility and metastable limit for a nonpolymorphic system, through sequential cooling (to induce primary nucleation at the metastable limit) and heating (to detect the saturation at the point of complete dissolution). Turbidity probes have also been utilized in similar manner,[18] more recently as part of a semiautomated system based on simultaneous measurements of transmission versus temperature profiles from parallel experiments.[19]

Other works[3,20−25] measured the solubility using in situ Attenuated Total Reflection-Fourier Transform Infrared (ATR-FTIR) spectroscopy from IR spectra of equilibrated slurries and appropriate calibration models to relate the spectra absorbances to solute concentration. In one such approach,[21] the calibration model is constructed by defining the intensity ratio of relevant ATR-FTIR spectra peaks as a calibration parameter to relate to solute concentration and temperature. Another approach[26] constructs the calibration model using multivariate statistical methods known as chemometrics, such as principal component regression (PCR) and partial least-squares (PLS). The measurement errors can be quantified in terms of the accuracy of the chemometrics predictions.[22]

This work demonstrates a semiautomated approach to determining the solubility of both forms of L-phenylalanine (L-phe) using ATR-FTIR spectroscopy, coupled with chemometrics, and FBRM in a single experiment. Such an approach has been demonstrated for nonpolymorphic systems;[15,16,27] to the best of the authors' knowledge, this paper is the first to present such an application for an enantiotropic dimorph system.

Experimental Section

Materials and Instrumentation. L-phe is an essential amino acid used as a food intermediate and pharmaceutical. Aqueous L-phe spectra were obtained by a Dipper-210 ATR immersion probe (Axiom Analytical) with ZnSe as the internal reflectance element attached to a Nicolet Protégé 460 FTIR spectrophotometer. A setting of 64 scans was used for each FTIR spectra. Ultrapure water at 23.5 °C was used for the background measurement. Although air has been used as a background in many past papers on ATR-FTIR spectroscopy, air near a crystallizer typically has variations in humidity that result in uncontrolled variation in the infrared spectra due to the strong absorbance of water in the mid-infrared region of the spectrum. The total counts of L-phe crystals in solution were measured every 20 s using Lasentec FBRM with version 6.0b12 of the FBRM Control Interface software. In addition, in situ images of the slurry were obtained using the Lasentec Particle Vision and Measurement (PVM) instrument. The solution temperature was controlled by ratioing hot and cold water to the jacket of a round-bottom flask with a control valve using a proportional-integral control system designed via internal model control[28−30] and was measured every 2 s using a Teflon-coated thermocouple attached to a Data Translation 3004 data acquisition board via a Fluke 80TK thermocouple module.[31−33] Powder X-ray diffraction (PXRD) patterns of L-phe crystals were collected offline using the Bruker General Area Detector Diffraction System (GADDS, Bruker AXS, Inc.) with Cu $K_{\alpha 1}$ and Cu $K_{\alpha 2}$ (weighted sum) radiation and step size 0.02°. The anhydrate form is orthorhombic while the monohydrate form is monoclinic; the space group is $P222_1$ for both.[10] Figure 2 shows PXRD patterns for both forms of L-phe; the characteristic peaks are consistent with a previous report.[10] L-phe crystals obtained commercially (>98.5%, Sigma Aldrich) were verified using PXRD to be pure anhydrate form; the characteristic peaks of the monohydrate form were not observed. These anhydrate-form crystals were used in the experiments without further purification. The monohydrate crystals were produced by rapidly cooling an initially undersaturated solution (0.045 g/g solvent) from 60.0 to 25.0 °C. The crystals were filtered, dried at 30.0 °C, and stored at room temperature with the polymorphic form confirmed using PXRD. The drying and storage temperatures have been previously verified to be sufficiently low that it did not lead to the dehydration of the monohydrate crystals.[10]

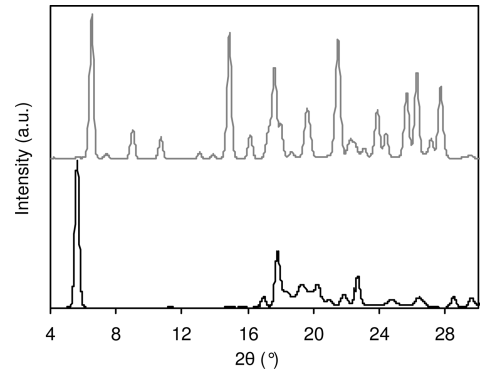

Figure 2. PXRD patterns of anhydrate (−) and monohydrate (gray line) forms of L-phe.

L-phe in aqueous solution is an enantiotropic pseudodimorph system where the anhydrate crystals (also denoted as the β-form[34,35]), which appear as platelets (Figure 3a), is the stable form above the transition temperature of 37.0 °C.[10] The penetration depth of the evanescent field at the ATR probe tip was sufficiently smaller than the anhydrate that the measured IR spectra measured the solution spectra with negligible interference from the crystals, as for most systems.[36] The monohydrate form (also denoted as the α-form[24,25]) appears as very fine needles (Figure 3b). Because the monohydrate needles were of dimensions comparable to the penetration depth of the evanescent field into the solution (~2.0 μm), the needles caused significant solid-phase interference on the measured IR spectra, making it difficult to determine solubility solely using ATR-FTIR spectroscopy. In particular, the inclusion of small crystals within the evanescent field results in the measured IR spectra indicating more solute than is actually present in solution.

Calibration for Solute Concentration. Different solute concentrations of L-phe and ultrapure water (approximately 400 g) were placed in a 500-ml jacketed round-bottom flask and heated until all the crystals dissolved, with the solution agitated by an overhead mixer with a stirring speed of 250 rpm. Table 1 lists the calibration samples. The solution was cooled at 0.5 °C/min while the IR spectra were collected. The measurements were stopped once crystals started to appear. The IR spectra in the range 1300−1415 cm^{-1} and the temperature were used to construct the calibration model. Figure 4 compares the representative IR spectra of L-phe solutions used for calibration and the resulting regression coefficients.

A calibration model relating the IR spectra and temperature to solute concentration was determined as described previously[25] using various chemometrics methods. The calculations were carried out using in-house MATLAB 5.3 (The Mathworks, Inc.) code except for partial least-squares (PLS) regression, which was from the PLS Toolbox 2.0. The correlation PCR[37] method with a noise level of 0.001 was selected that gave the smallest prediction interval of ±0.00051 g/g solvent while being

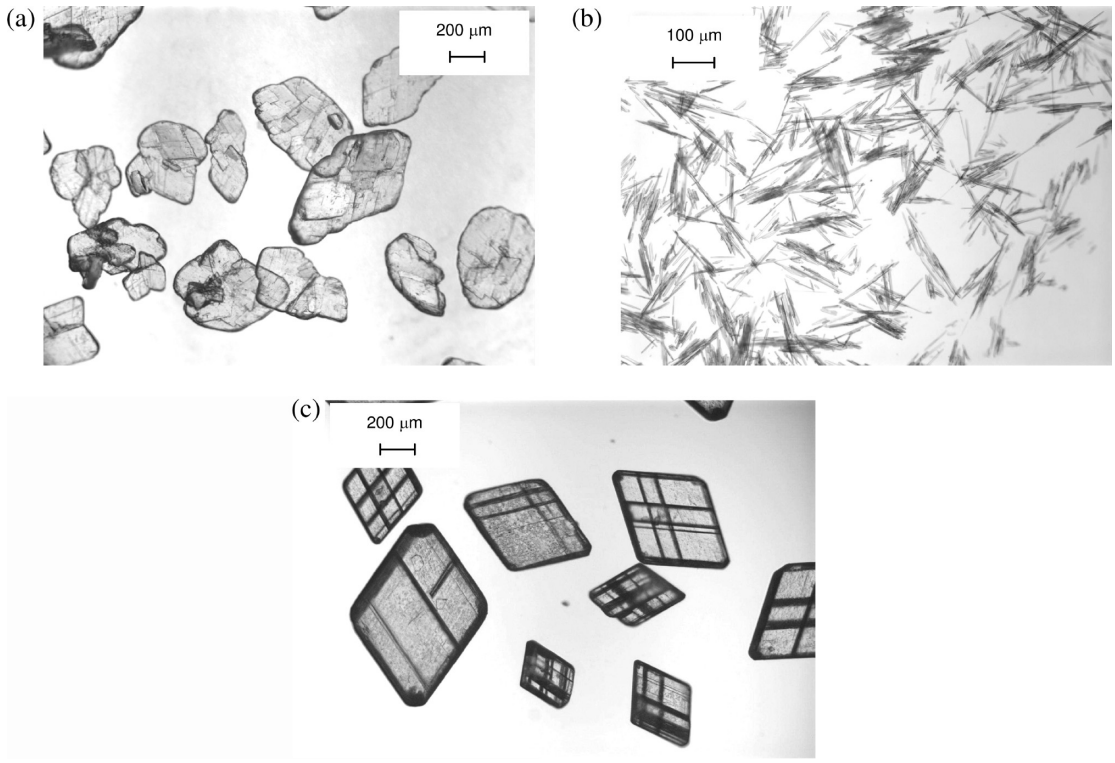

Figure 3. Microscopy images of L-phe: (a) anhydrate form as is from Sigma Aldrich (>98.5%), (b) monohydrate form, and (c) the anhydrate form with a more well-defined habit as rhombic platelets obtained through recrystallization.

Table 1. ATR-FTIR Calibration Samples

calibration sample	solute concentration (g/g solvent)	T range (°C)	no. of spectra
Cs1	0.02407	26.9−19.5	12
Cs2	0.03004	38.9−23.0	22
Cs3	0.03702	49.9−35.0	20
Cs4	0.04402	60.8−43.1	22
Cs5	0.05025	67.6−51.0	19

consistent with the accuracy of the solubility data. The calibration model had the form

$$C = \sum_{j=1300}^{1415} w_j a_j + w_T T + w_0 \quad (1)$$

where C is the solute concentration (g/g solvent), a_j is the absorbance at frequency j (cm^{-1}), T is the temperature (°C), and w_j, w_T, and w_0 are regression coefficients.

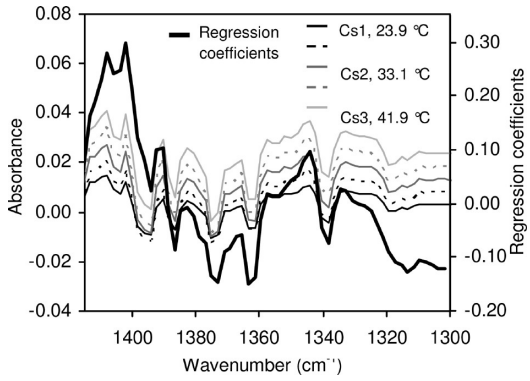

Figure 4. Representative ATR-FTIR spectra of the calibration samples and regression coefficients of the calibration model relating absorbance to solute concentration. The regression coefficients for the temperature and the intercept are not shown.

Solubility Measurements. The solubility of both forms of L-phe was determined using two methods. In Method 1, the solubility for each form was determined separately through addition of excess crystals of a specific form to create a saturated slurry, while in the semiautomated approach denoted as Method 2, the solubility of both forms was determined from a single experiment. The solvent mass used in both methods was ~400 g, and the stirring speed of the overhead mixer was maintained at 300 rpm. To shorten the time required to achieve saturation, anhydrate-form crystals of smaller sizes (<250 μm) were used.

Method 1: Solubility Measurements from Separate Experiments. For the anhydrate form, the IR spectra of the slurry were collected at different temperature points ranging from 25.0 to 60.0 °C. The solute concentration profile was tracked using the aforementioned calibration model, and the required equilibration time at each evaluated temperature point was decided based on the total counts/sec profile measured by FBRM. The equilibrium solute concentration was first deter-

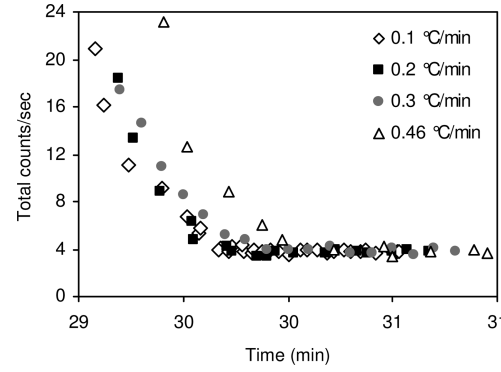

Figure 5. Total counts/sec profiles as a function of temperature at different heating rates. The nonzero baseline value was due to the presence of bubbles caused by the high stirring rate.

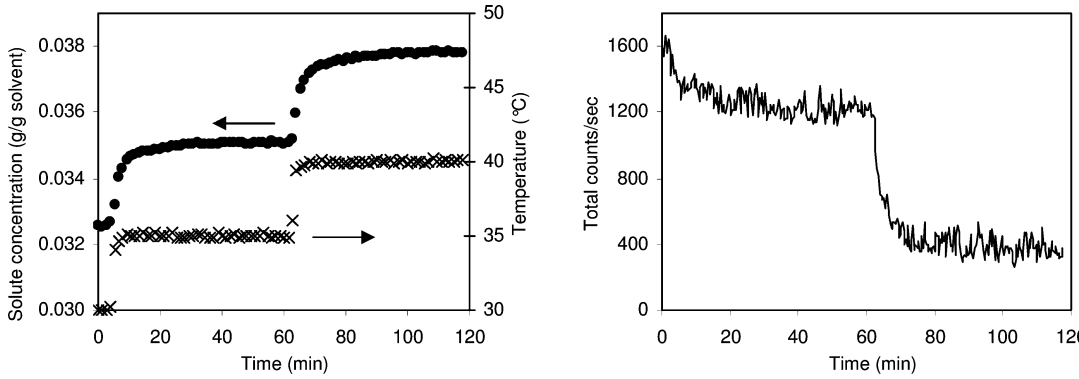

Figure 6. Solute concentration and temperature profiles (left) and total counts/sec profile (right) in the solubility experiment for anhydrate L-phe crystals using Method 1.

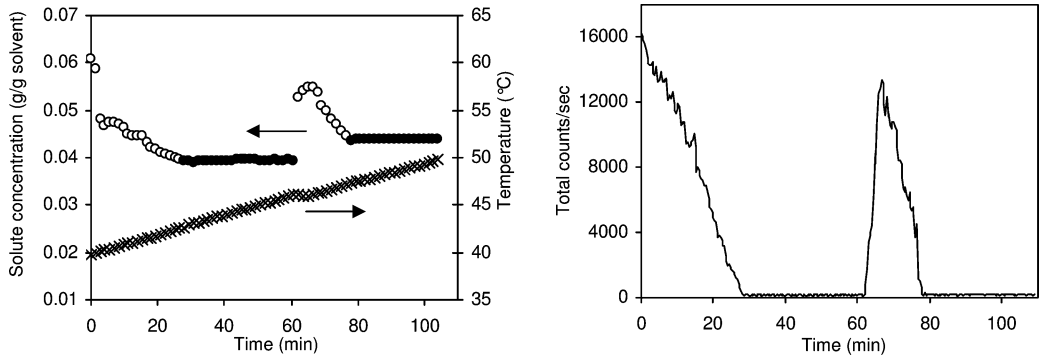

Figure 7. Solute concentration and temperature profiles (left) and total counts/sec profile (right) in the solubility experiment for monohydrate form L-phe using Method 1. The open circles (left) indicate erroneous concentration values as indicated by the apparent decrease in solute concentration during an increase in temperature, which are timed exactly with the appearance of crystals (right); the solid circles indicate correct measurements.

mined at a low temperature and the slurry temperature was increased in stages to determine the solubility at higher temperatures. When necessary, more anhydrate-form crystals were added in excess so that saturation could be achieved at all the evaluated temperature points.

For the monohydrate, the solubility could not be determined from IR measurement of the equilibrated slurry due to significant solid-phase interference that resulted in erroneous measurement even at low slurry density. Instead, the slurry was heated slowly at 0.1 °C/min after equilibration, while tracking the solute concentration and total counts/sec from the FBRM. The saturation temperature and the corresponding solute concentration were determined at the lowest temperature (at the earliest time point) where the counts/sec profiles approached a constant value, indicating complete dissolution. The solubility can be determined reliably using the above approach only if the heating rate is sufficiently slow relative to solids dissolution that the slurry was always in equilibrium as the temperature increased. In a preliminary experiment, different heating rates were evaluated to ensure that the heating rate used in the solubility measurement was sufficiently slow to maintain equilibrium. At the heating rates of 0.1 and 0.2 °C/min, the counts/sec fell to a plateau value at the same temperature, while this plateau value was reached for higher temperatures at larger heating rates (Figure 5). The initial mass of monohydrate-form crystals in the slurry equilibrated at 21.0 °C was identical in these four runs. This showed that the heating rate of 0.1 °C/min was sufficiently slow relative to solid dissolution for equilibrium to be maintained as the temperature increased. The solubility measurements obtained by FBRM were performed twice for each evaluated temperature point.

Method 2: Single-Experiment Semiautomated Approach. The solubility of the anhydrate form at the initial temperature was determined from a slurry in a similar manner to Method 1. The slurry was then heated to dissolve all the excess anhydrate crystals, and the solution was cooled to a sufficiently low temperature. Small quantities of monohydrate-form seed crystals were added to induce the nucleation of this form. Upon sufficient crystallization of the monohydrate form, the slurry was heated at 0.1 °C/min, and the solubility was determined upon complete dissolution as in Method 1. The cycle was repeated at higher temperatures after addition of anhydrate crystals to make a slurry.

Monitoring Polymorph Form. Methods 1 and 2 are facilitated by online or off-line measurement of the polymorph form. A simple off-line approach is to collect small

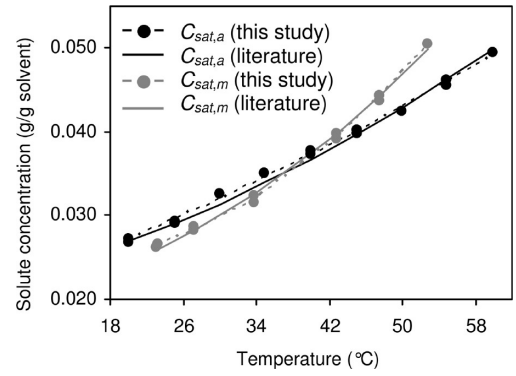

Figure 8. L-phe solubility curves compared to published data[10] for the anhydrate form, $C_{sat,a}$, and monohydrate form, $C_{sat,m}$. Crossover temperature measured as 37 °C.

Table 2. Fitting Parameters for Anhydrate and Monohydrate Form L-Phe Solubility Curves

fitting parameters	anhydrate form - this study	anhydrate form - literature[10]	monohydrate form - this study	monohydrate form - literature[10]
$b_{0,i}$	1.854×10^{-2}	2.043×10^{-2}	2.595×10^{-2}	1.949×10^{-2}
$b_{1,i}$	3.890×10^{-4}	2.394×10^{-4}	-3.188×10^{-4}	5.169×10^{-5}
$b_{2,i}$	1.987×10^{-6}	4.211×10^{-6}	1.479×10^{-5}	9.900×10^{-6}

samples using a robotic sampling system and quantifying the ratio of polymorphic forms by powder X-ray diffraction.[38] Online techniques for measuring polymorph form[39] include Raman spectroscopy,[11,20,40−46] in situ X-ray diffraction,[47] laser backscattering,[48] and process video microscopy.[49] Raman spectroscopy is usually applicable for compounds that do not fluoresce and process video microscopy is only applicable to polymorphs with different shapes. Process video microscopy was applied in this work as the crystals of the two polymorphs are vastly different in shape (Figure 2); this method could be replaced by any reliable approach for quantifying form identity, depending on the particular characteristics of the system.

Results and Discussion

Method 1. For the anhydrate form, the solubility was determined from in situ solute concentration measurement of slurry equilibrated at various temperatures. For example, Figure 6 shows the solute concentration and total counts/sec profiles of a slurry containing anhydrate L-phe crystals initially equilibrated at 30 °C, approaching saturation after two temperature ramps to 35 and 40 °C. The plateau in counts/sec reached after 30 min in both cases was taken as indicative of saturation. This corresponded to solute concentrations of 0.03505 and 0.03777 g/g solvent at 35 and 40 °C, respectively.

The solubility of the monohydrate form was determined from slow heating of equilibrated slurry due to interference of the monohydrate-form crystals on the IR measurements. As the monohydrate slurry was heated at 0.1 °C/min (Figure 7a), the counts/sec initially decreased due to dissolution of the solid phase (Figure 7b), and the amount of interference on the ATR probe also reduced. When the solid phase was completely dissolved as detected by the total counts/sec dropping to zero, the solute concentration was correctly estimated. The equilibrium solute concentration was determined at the lowest temperature (which would be the saturation temperature) where both the concentration and counts/sec did not exhibit further changes due to complete dissolution. The solubility was 0.03920 g/g solvent and the temperature at this time point (~28 min) was 42.8 °C. The next slurry was prepared by adding more monohydrate crystals at 62 min. After equilibration, the same heating rate was applied. The saturation temperature was detected at 47.6 °C (at ~78 min) and the corresponding solute concentration was 0.04349 g/g solvent. The estimated equilibrium solute concentration in both cases was consistent with that calculated based on the total crystal mass added into the slurry. The solubility of monohydrate form was determined at other temperatures in similar manner. As shown in Figure 8, there is good agreement between the solubility curves of both forms of L-phe determined using Method 1 with available solubility data.[10] The largest discrepancy for the anhydrate form amounted to only −0.00092 g/g solvent (−1.8%) while that for the monohydrate form was 0.00053 g/g solvent (1.1%). Although the dissimilarities are statistically significant given that they exceeded the prediction interval of the calibration model, it could be attributed to differences in the purity of the solute and solvent used. Multiple measurements are shown in Figure 8 at each temperature, which indicate a standard deviation in the solute concentration measurements of less than 0.001 g/g solvent.

To compare with the analytical expressions given in ref 10 the solubility curves were fit to

$$C_{\mathrm{sat},i} = b_{0,i} + b_{1,i}T + b_{2,i}T^2 \quad (2)$$

where i denotes anhydrate or monohydrate form and $C_{\mathrm{sat},i}$ (g/g solvent) is the solubility (Table 2). The maximum deviation of the experimental data points from the fitted solubility curves (0.00050 and −0.00049 g/g solvent for the anhydrate and monohydrate forms, respectively) were within the prediction interval.

Method 2. The semiautomated approach (Method 2) combined both procedures in Method 1 to measure the solubility of both forms of L-phe in a single experiment. Figure 9 illustrates two operation cycles in the low and middle temperature range for this approach. In Cycle 1, the solubility of the anhydrate form was determined from an equilibrated slurry (part a) similar to that described in Method 1. The system was then heated to

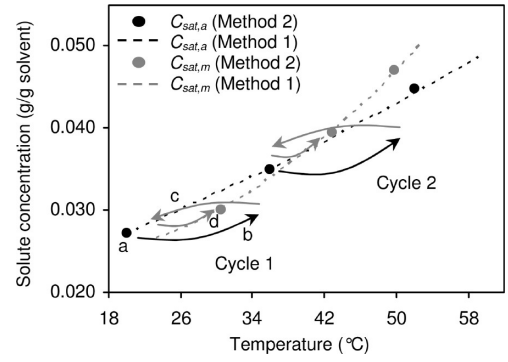

Figure 9. Schematic of Method 2 and L-phe solubility points using Method 2 compared to the fitted solubility curves from Method 1.

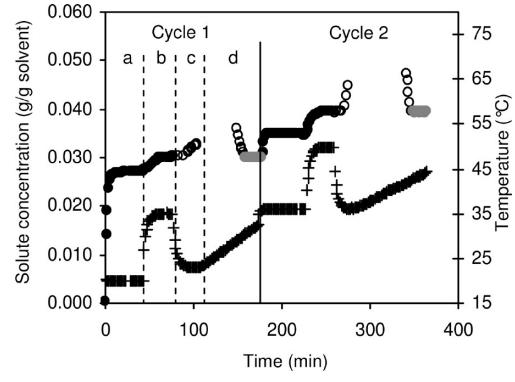

Figure 10. Solute concentration, anhydrate form (●) and monohydrate form (filled gray circle), and temperature (+) profiles in the solubility experiment using Method 2. The concentration profile is not shown entirely for parts (c) and (d) because of erroneous measurement due to interference from monohydrate needles. The open circles indicate erroneous concentration values associated with the gray total counts/sec peaks in Figure 11, and the solid circles indicate correct measurements.

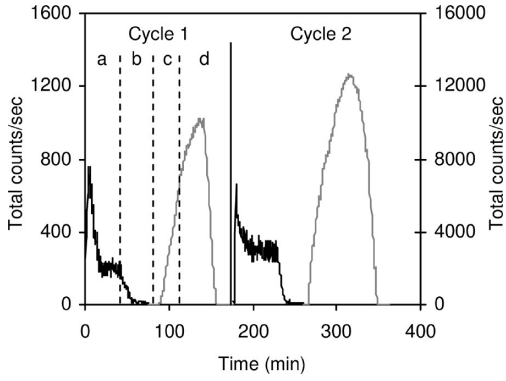

Figure 11. Total counts/sec profile in the solubility experiment using Method 2 with the anhydrate form (−) referencing the left axis and the monohydrate form (gray line) referencing the right axis. Time lag in reduction in count/sec in phase d believed to be due to some crystals temporarily stuck to FBRM probe tip.

dissolve the anhydrate form (part b) and cooled to generate supersaturation to nucleate the monohydrate form (part c). Seed crystals were added to ensure nucleation of the correct form as well as to expedite the recrystallization process. Upon sufficient recrystallization, the slurry was heated at 0.1 °C/min and the solubility was determined at the point of complete dissolution (part d), similar to that described in Method 1. The slurry was then heated to the initial temperature for Cycle 2, and excess amount of the anhydrate crystals was added before starting this cycle. The solute concentration, temperature, and counts/sec profiles during both cycles are shown in Figures 10 and 11. The first plateau in the concentration and total counts/sec profiles in part (a) (similar to that in Figure 6) indicates saturation of the anhydrate crystal slurry at 20 °C and 0.02722 g/g solute.

The subsequent plateau in part (b) corresponds to complete dissolution of anhydrate solids upon heating to 35.0 °C. Subsequent cooling to 23.0 °C and seeding with small amounts of monohydrate crystals resulted in the nucleation of this form, indicated by the increase in the total counts in part (c). At the start of heating in part (d), the total counts continued to increase because the slurry was still supersaturated, but decreased eventually when solids dissolved with increasing temperature. The lowest temperature at which the solute concentration (0.03013 g/g solvent) did not exhibit further changes due to complete dissolution was taken as the saturation temperature, 30.6 °C. The total counts/sec (Figure 11) fell to a constant value upon reaching the saturation temperature, similar to Figure 7. In situ video microscopy images (Figure 12) were monitored to ensure that crystals of the correct polymorph were obtained during solubility measurements.

Similar analysis for Cycle 2 based on the three profiles gave the following solubility values: 0.03497 g/g solute at 36.0 °C (anhydrate form) and 0.03935 g/g solvent at 42.8 °C (monohydrate form). The obtained solubility values were consistent with the solubility curves determined using Method 1 (Figure 8). Other solubility points were determined in the same manner at different temperatures. The solubility measurement of the metastable form (i.e., anhydrate and monohydrate forms below

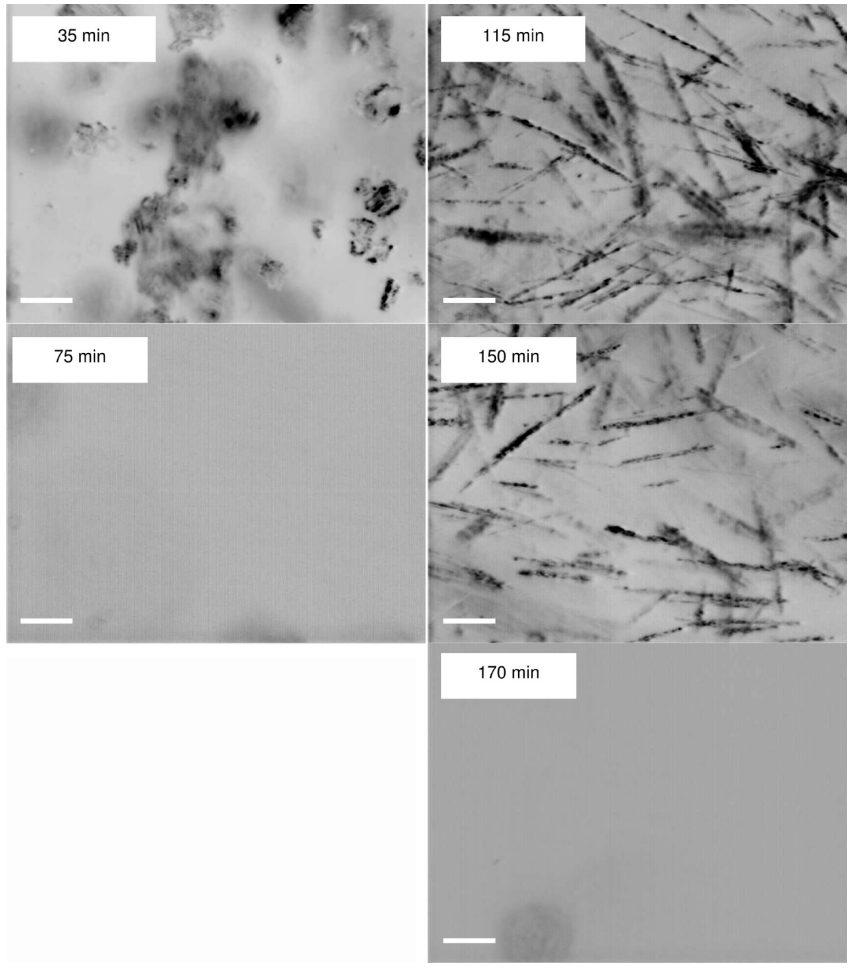

Figure 12. PVM images from the solubility experiment using Method 2 (scale bar 100 μm): at the anhydrate form saturation, the recrystallization of the monohydrate form, and the eventual dissolution.

and above the transition temperature, respectively) using the above methods applies only if the dissolution of this form is relatively faster than its transformation to the stable modification so that equilibrium with respect to the metastable form is achievable.[10] This occurs for the L-phe for the studied temperature range,[10] has been observed in other polymorphic systems,[20] and is expected to be fairly common since nucleation of the stable form from a slurry of metastable crystals requires crossing energy barriers to molecular ordering whereas dissolution does not.

In this semiautomated procedure, the temperature cycle was automated by following a preprogrammed profile, and the addition of excess anhydrate crystals and monohydrate seeds were performed manually at various stages of the sequence.[50] This was necessary to produce a slurry containing only a single polymorph in a reasonable time. Previous works[15,16] on fully automated approaches in nonpolymorphic systems relied on primary nucleation to create a slurry, but this form of nucleation may not be feasible for polymorphic systems because it may lead to concomitant polymorphs. The procedure allowed the solubility determination of both forms in a single experiment, reducing time and labor. This is also advantageous because handling of recrystallized solid phases is minimized to reduce the risk of dehydration, especially for hydrates, during drying or storage.

Conclusions

A semiautomated procedure for measuring the solubility of both enantiotropes in a dimorphic system in a single experiment was developed using ATR-FTIR spectroscopy for in situ measurement of solute concentration and FBRM to measure particle counts. This was applied to enantiotropic pseudodimorph L-phenylalanine. The solubility of the anhydrate form was determined by measuring the solute concentration isothermally at saturated conditions. The time required to reach saturation was determined from the asymptotic behavior of both the solute concentration and total counts/sec profiles. Due to significant interference from the solid phase on the IR measurement, the solubility of the monohydrate form was determined from the dissolution of the slowly heated monohydrate slurry. The saturation temperature and the corresponding solute concentration were determined at the lowest temperature where the particle counts and solute concentration profiles approached a constant value, indicating complete dissolution. This approach requires less materials and manual labor compared to other techniques such as the gravimetric methods.

Acknowledgment

The authors thank Scott Wilson from the George L. Clark X-ray facility for the PXRD data collection, Mitsuko Fujiwara for comments on the manuscript, and the Singapore Agency for Science, Technology, and Research for financial support.

Literature Cited

(1) Threlfall, T. Crystallization of polymorphs: Thermodynamic insight into the role of solvent. *Org. Process. Res. Dev.* **2000**, *4*, 384–390.

(2) Beckmann, W. Seeding the desired polymorph: Background, possibilities, limitations, and case studies. *Org. Process. Res. Dev.* **2000**, *4*, 372–383.

(3) Lewiner, F.; Klein, J. P.; Puel, F.; Fevotte, G. On-line ATR FTIR measurement of supersaturation during solution crystallization processes. Calibration and applications on three solute/solvent systems. *Chem. Eng. Sci.* **2001**, *56*, 2069–2084.

(4) Haleblian, J.; McCrone, W. Pharmaceutical applications of polymorphism. *J. Pharm. Sci.* **1969**, *58*, 911–929.

(5) Higuchi, W. I.; Lau, P. K.; Higuchi, T.; Shell, J. W. Polymorphism and drug availability—Solubility relationships in methylprednisolone system. *J. Pharm. Sci.* **1963**, *52*, 150–15.

(6) Grunenberg, A.; Henck, J. O.; Siesler, H. W. Theoretical derivation and practical application of energy temperature diagrams as an instrument in preformulation studies of polymorphic drug substances. *Int. J. Pharm.* **1996**, *129*, 147–158.

(7) Umeda, T.; Ohnishi, N.; Yokoyama, T.; Kuroda, T.; Kita, Y.; Kuroda, K.; Tatsumi, E.; Matsuda, Y. Studies on drug nonequivalence 0.15. Physicochemical properties and isothermal transition of acetazolamide polymorphs. *Chem. Pharm. Bull.* **1985**, *33*, 3422–3428.

(8) Behme, R. J.; Brooke, D. Heat of fusion measurement of a low melting polymorph of carbamazepine that undergoes multiple-phase changes during differential scanning calorimetry analysis. *J. Pharm. Sci.* **1991**, *80*, 986–990.

(9) Urakami, K.; Shono, Y.; Higashi, A.; Umemoto, K.; Godo, M. A novel method for estimation of transition temperature for polymorphic pairs in pharmaceuticals using heat of solution and solubility data. *Chem. Pharm. Bull.* **2002**, *50*, 263–267.

(10) Mohan, R.; Koo, K. K.; Strege, C.; Myerson, A. S. Effect of additives on the transformation behavior of L-phenylalanine in aqueous solution. *Ind. Eng. Chem. Res.* **2001**, *40*, 6111–6117.

(11) Ono, T.; Kramer, H. J. M.; Horst, J. H.; Jansens, P. J. Process modeling of the polymorphic transformation of L-glutamic acid. *Cryst. Growth Des.* **2004**, *4*, 1161–1167.

(12) Gracin, S.; Rasmuson, A. C. Polymorphism and crystallization of p-aminobenzoic acid. *Cryst. Growth Des.* **2004**, *4*, 1013–1023.

(13) Luk, C.-W. J.; Rousseau, R. W. Solubilities of and transformations between the anhydrous and hydrated forms of L-serine in water-methanol solutions. *Cryst. Growth Des.* **2006**, *6*, 1808–1812.

(14) Maruyama, S.; Ooshima, H.; Kato, J. Crystal structures and solvent-mediated transformation of Taltireline polymorphs. *Chem. Eng. J.* **1999**, *75*, 193–200.

(15) Liotta, V.; Sabesan, V. Monitoring and feedback control of supersaturation using ATR-FTIR to produce an active pharmaceutical ingredient of a desired crystal size. *Org. Process Res. Dev.* **2004**, *8*, 488–494.

(16) Barrett, P.; Glennon, B. Characterizing the metastable zone width and solubility curve using lasentec FBRM and PVM. *Chem. Eng. Res. Des.* **2002**, *80*, 799–805.

(17) Togkalidou, T.; Braatz, R. D.; Johnson, B. K.; Davidson, O.; Andrews, A. Experimental design and inferential modeling in pharmaceutical crystallization. *AIChE J.* **2001**, *47*, 160–168.

(18) Parsons, A. R.; Black, S. N.; Colling, R. Automated measurement of metastable zones for pharmaceutical compounds. *Chem. Eng. Res. Des.* **2003**, *81*, 700–704.

(19) Yi, Y.; Hatziavramidis, D.; Myerson, A. S.; Waldo, M.; Beylin, V. G.; Mustakis, J. Development of a small-scale automated solubility measurement apparatus. *Ind. Eng. Chem. Res.* **2005**, *44*, 5427–5433.

(20) Fujiwara, M.; Chow, P.; Ma, D.; Braatz, R. D. Paracetamol crystallization using laser backscattering and ATR-FTIR spectroscopy: Metastability, agglomeration, and control. *Cryst. Growth Des.* **2002**, *2*, 363–370.

(21) Schöll, J.; Bonalumi, D.; Vicum, L.; Mazzotti, M.; Müller, M. In situ monitoring and modeling of the solvent-mediated polymorphic transformation of L-glutamic acid. *Cryst. Growth Des.* **2006**, *6*, 881–891.

(22) Grön, H.; Borissova, A.; Roberts, K. J. In-process ATR-FTIR spectroscopy for closed-loop supersaturation control of a batch crystallizer producing monosodium glutamate crystals of defined size. *Ind. Eng. Chem. Res.* **2003**, *42*, 198–206.

(23) Dunuwila, D. D.; Berglund, K. A. ATR FTIR spectroscopy for in situ measurement of supersaturation. *J. Cryst. Growth* **1997**, *179*, 185–193.

(24) Pöllänen, K.; Häkkinen, A.; Reinikainen, S.-P.; Louhi-Kultanen, M.; Nyström, L. A study on batch cooling crystallization of sulphathiazole - Process monitoring using ATR-FTIR and product characterization by automated image analysis. *Chem. Eng. Res. Des.* **2006**, *84*, 47–51.

(25) Fevotte, G. New perspectives for the on-line monitoring of pharmaceutical crystallization processes using in situ infrared spectroscopy. *Int. J. Pharm.* **2002**, *241*, 263–278.

(26) Togkalidou, T.; Fujiwara, M.; Patel, S.; Braatz, R. D. Solute concentration prediction using chemometrics and ATR-FTIR spectroscopy. *J. Cryst. Growth* **2001**, *231*, 534–543.

(27) Zhou, G. X.; Fujiwara, M.; Woo, X. Y.; Rusli, E.; Tung, H. H.; Starbuck, C.; Davidson, O.; Ge, Z.; Braatz, R. D. Direct design of pharmaceutical antisolvent crystallization through concentration control. *Cryst. Growth Des.* **2006**, *6* (4), 892–898.

(28) Morari, M.; Zafiriou, E. *Robust Process Control*; Prentice Hall: Englewood Cliffs, NJ, 1989.

(29) Braatz, R. D. Internal Model Control. In *The Control Handbook*; Levine, W. S., Ed.; CRC Press, Boca Raton, FL, 1995, 215−224.

(30) Horn, I. G.; Arulandu, J. R.; Gombas, C. J.; VanAntwerp, J. G.; Braatz, R. D. Improved filter design in internal model control. *Ind. Eng. Chem. Res.* **1996**, *35*, 3437–3441.

(31) Fujiwara, M.; Nagy, Z. K.; Chew, J. W.; Braatz, R. D. First-principles and direct design approaches for the control of pharmaceutical crystallization. *J. Process Control* **2005**, *15*, 493–504.

(32) Nagy, Z. K.; Fujiwara, M.; Chew, J. W.; Braatz, R. D. Comparative performance of concentration and temperature controlled batch crystallizations. *J. Process Control* **2008**, *18*, 399–407.

(33) Togkalidou, T.; Tung, H.-H.; Sun, Y.; Andrews, A.; Braatz, R. D. Parameter estimation and optimization of a loosely-bound aggregating pharmaceutical crystallization using in-situ infrared and laser backscattering measurements. *Ind. Eng. Chem. Res.* **2004**, *43*, 6168–6181.

(34) Yano, J.; Furedi-Milhofer, H.; Wachtel, E.; Garti, N. Crystallization of organic compounds in reversed micelles. II. Crystallization of glycine and L-phenylalanine in water-isooctane−AOT microemulsions. *Langmuir* **2000**, *16*, 10005–10014.

(35) Khawas, B. X-ray study of L-phenylalanine dimorph and D-tyrptophane. *Indian J. Phys. A* **1985**, *59*, 219–226.

(36) Lewiner, F.; Klein, J. P.; Puel, F.; Fevotte, G. Improving batch cooling seeded crystallization of an organic weed-killer using on-line ATR FTIR measurement of supersaturation. *J. Cryst. Growth* **2001**, *226*, 348–362.

(37) Xie, Y.-L.; Kalivas, J. H. Evaluation of principal component selection methods to form a global prediction model by principal component regression. *Anal. Chim. Acta* **1997**, *348*, 19–27.

(38) Bernstein, J.; Henck, J.-O. Pharmaceuticals. In *Industrial Applications of X-ray Diffraction*; Chung, F. H., Smith, D. K., Ed.; Marcel Dekker AG: New York, 2000, 527−538.

(39) ATR-FTIR spectroscopy is not effective for on-line measurement of polymorph crystals in solution.

(40) Starbuck, C.; Spartalis, A.; Wai, L.; Wang, J.; Fernandez, P.; Lindemann, C. M.; Zhou, G.; Ge, Z. Process optimization of a complex pharmaceutical polymorphic system via in situ Raman spectroscopy. *Cryst. Growth Des.* **2002**, *2*, 515–522.

(41) Hu, Y.; Liang, J. K.; Myerson, A. S.; Taylor, L. S. Crystallization monitoring by Raman spectroscopy: Simultaneous measurement of desupersaturation profile and polymorphic form in flufenamic acid systems. *Ind. Eng. Chem. Res.* **2005**, *44*, 1233–1240.

(42) Fevotte, G. In situ raman spectroscopy for in-line control of pharmaceutical crystallization and solids elaboration processes: A review. *Chem. Eng. Res. Des.* **2007**, *85*, 906–920.

(43) Tamagawa, R. E.; Miranda, E. A.; Berglund, K. A. Raman spectroscopic monitoring and control of aprotinin supersaturation in hanging-drop crystallization. *Cryst. Growth Des.* **2002**, *2*, 263–267.

(44) Tamagawa, R. E.; Miranda, E. A.; Berglund, K. A. Simultaneous monitoring of protein and $(NH_4)_2SO_4$ concentrations in aprotinin hanging-drop crystallization using Raman spectroscopy. *Cryst. Growth Des.* **2002**, *2*, 511–514.

(45) Qu, H.; Alatalo, H.; Hatakka, H.; Kohonen, J.; Louhi-Kultanen, M.; Reinikainen, S.-P.; Kallas, J. Raman and ATR FTIR spectroscopy in reactive crystallization: Simultaneous monitoring of solute concentration and polymorphic state of the crystals. *J. Cryst. Growth* **2009**, *311*, 3466–3475.

(46) Caillet, A.; Puel, F.; Fevotte, G. In-line monitoring of partial and overall solid concentration during solvent-mediated phase transition using Raman spectroscopy. *Int. J. Pharm.* **2006**, *307*, 201–208.

(47) MacCalman, M. L.; Roberts, K. J.; Kerr, C.; Hendriksen, B. Online processing of pharmaceutical materials using in-situ x-ray-diffraction. *J. Appl. Crystallogr.* **1995**, *28*, 620–622.

(48) Barthe, S. C.; Grover, M. A.; Rousseau, R. W. Observation of polymorphic change through analysis of FBRM data: Transformation of paracetamol from form II to form I. *Cryst. Growth Des.* **2008**, *8*, 3316–3322.

(49) O'Sullivan, B.; Barrett, P.; Hsiao, G.; Carr, A.; Glennon, B. *Org. Process Res. Dev.* **2003**, *7*, 977–982.

(50) This manual step can be replaced by a robotic system for adding crystals to the system.

Received for review April 1, 2010
Revised manuscript received October 27, 2010
Accepted October 28, 2010

IE100794H